

Structure and defects of vapor-phase-grown diamond nanocrystals

X. Jiang^{a)}

Fraunhofer-Institut für Schicht- und Oberflächentechnik, Bienroder Weg 54E, D-38108 Braunschweig, Germany

C. L. Jia

Institut für Festkörperforschung, Forschungszentrum Jülich GmbH, D-52425 Jülich, Germany

(Received 4 October 2001; accepted for publication 5 January 2002)

Diamond nanocrystalline films are prepared by the ion bombardment-assisted gas vapor synthesis technique. The phase quality, morphology and microstructure of the films are investigated by means of Raman spectroscopy, scanning electron microscopy, and high-resolution transmission electron microscopy. The grain size in the film ranges from several nanometers to several tens of nanometers. There is a high density of lattice defects, mainly stacking faults and twin boundaries in the nanocrystals. Lattice distortions, vacancies, and dislocations are observed. The growth of nanocrystals and the mechanism of defect formation are discussed in light of the ion impact effect.

© 2002 American Institute of Physics. [DOI: 10.1063/1.1458071]

Nanocrystalline (nc) films with extremely high grain boundary density have been attracting rapidly increasing interest that focuses on the design of optimum materials by reducing grain dimensions and on the new properties now achievable.¹

Nucleation and growth of nc diamond films was first achieved on scratched Si substrates from hydrogen-poor argon plasma using fullerenes as growth precursors.² Phase-pure diamond is grown at very low hydrogen concentrations.³ Unique diamond films with grains of nanometer size exhibit a broad range of fascinating mechanical, electrical, and optical properties.⁴ By adding nitrogen to a plasma with a high methane concentration, films that exhibit a nanocrystalline appearance were also obtained.⁵

Based on the effect of ion-bombardment-induced high frequency secondary nucleation another method for the synthesis of diamond nanocrystals was reported recently.^{6,7} For modified diamond film, growth in microwave plasma chemical vapor deposition (MWCVD) ion bombardment of different energy ranges at different substrate temperatures has been investigated.⁸ By means of ion bombardment induced by negatively biasing the substrate at voltage above 80 V the grain size of the films begins to decrease and nc diamond films can be obtained at a bias voltage that exceeds -140 V. Due to shallow ion penetration at the subsurface region (ion subplantation) the nc films prepared show high intrinsic compressive stress and attractive electron emission properties.^{9,10}

In comparison to other nc materials, the structural properties of nc diamond have been studied little. The defect structure within the nanocrystal, in particular, has not been reported. In this letter we report investigations of the crystal structure and defects of nc diamond films prepared by a MWCVD process via ion bombardment using scanning electron microscopy (SEM) and high-resolution transmission electron microscopy (HRTEM), and studies of the phase quality using Raman spectroscopy (RS). Much attention was

paid to the influence of ion bombardment on the film structure and crystal defects.

A $1\text{ }\mu\text{m}$ thick film consisting of diamond nanocrystals was deposited on a 2 in. *n*-type (001) silicon wafer by applying negative bias potential of -140 V to the substrate at 780°C and 25 mbar. The microwave plasma power was kept at 800 W. A pure methane-in-hydrogen gas mixture with a methane concentration of 0.4 at. % was used as the process gas. No Ar was introduced into the plasma. Figure 1 shows a SEM image of the morphology of a typical nc film. The film shows a structure that is made up of nanocrystalline clusters. An average grain size smaller than 40 nm can be roughly estimated. The film surface is smooth, showing an average surface roughness of 5 nm as measured with a surface profilometer.

To confirm the deposition of diamond and to study the phase purity of the films, micro-Raman spectroscopy was performed. The Raman spectrum was obtained with a laser spot size approximately $20\text{ }\mu\text{m}$ in diameter on the samples. Figure 2 shows the Raman spectra obtained from samples prepared with and without substrate biasing. The formation of diamond phase is not only demonstrated by the occurrence of the first order diamond line at $\lambda = 1334\text{ cm}^{-1}$ for the microcrystalline (mc) film, but also for the nc diamond film prepared at -140 V. We also observed a broad peak at

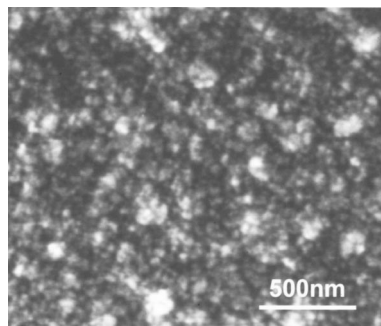


FIG. 1. SEM image of the morphology of the film prepared under -140 V substrate bias voltage.

^{a)}Electronic mail: jiang@ist.fhg.de

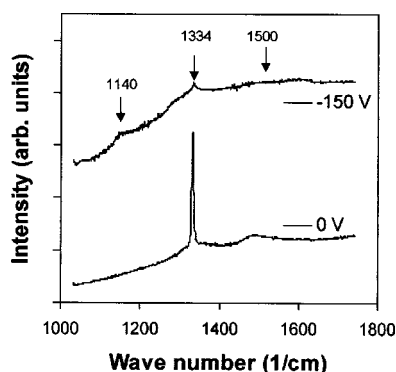


FIG. 2. Raman spectra of a nanostructured diamond film and a microcrystalline film.

around 1140 cm^{-1} which was suggested to arise either from the small grain size or from disorder in a tetrahedrally bonded carbon network. A low broad signal from 1400 to 1600 cm^{-1} caused by sp^2 -bonded carbon was also detected. The diamond line for the nc film is shifted from $\lambda = 1334\text{ cm}^{-1}$ for the mc film to a higher wave number ($\lambda = 1337\text{ cm}^{-1}$). Correspondingly, the full width at half maximum (FWHM) of the line increases from 5.3 to 13 cm^{-1} . These are result of the large compressive film stress and crystal defects produced at $V_b = -140\text{ V}$. We observed *in situ* the development of film stress during film deposition by the bending beam method with two laser beams and found that the films of $1\text{ }\mu\text{m}$ thickness may have compressive stress as high as 4 GPa .⁷

Electron microscopic investigation showed that the grain size of these nanocrystals ranges from several nanometers to several tens of nanometers. Figure 3 shows a high-resolution plane-view lattice image of the film's area including the small nanocrystals. Diamond $\{111\}$ lattice fringes with spacing of 0.206 nm are clearly visible. In most cases, the small nanocrystals have a spherical shape. Regions without lattice fringe contrast can be seen between these small crystals (in the grain boundary area). These regions may be occupied by diamond grains which are not in a proper orientation to show the lattice fringe in the image as well as by a secondary phase like amorphous carbon which is revealed by Raman analysis. The average particle size shown in this image is less than 10 nm .

The lattice image shown in Fig. 3 provides us with strong evidence that diamond nanocrystals can be grown by the ion-bombardment-assisted process. A detailed investigation reveals that the diamond grains are highly faulted. The

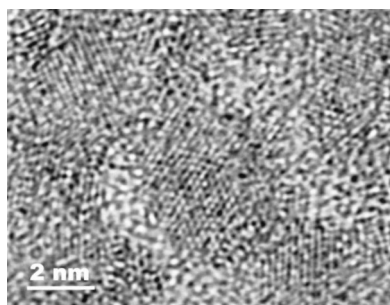


FIG. 3. Plane-view lattice image of the nanodiamond film. The $\{111\}$ lattice fringes of diamond are clearly seen.

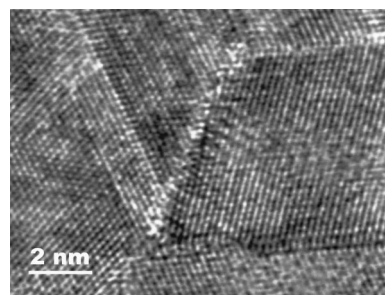


FIG. 4. Lattice defects frequently observed in nanodiamond crystals.

most common defects in coarse-grained diamond films, twin boundaries ($\Sigma=3$) and stacking faults, are frequently observed in these nanocrystals as shown in Fig. 4. The quintuplet twin structure often found in the mc film¹¹ is also observed in nanodiamond crystal. Figure 5 shows a quintuplet nanotwin structure. It is known that for a cubic structure such as silicon or diamond the $\{111\}$ twinning angle between two adjacent twin variants is in equilibrium 70.53° .^{11,12} After fivefold twinning there is still a mismatch angle of $360^\circ - 70.53^\circ \times 5 = 7.35^\circ$ between the first variant and the fifth variant. In this case, a $\Sigma=81$ boundary was found which appeared to accommodate the mismatch angle.¹¹ Due to the extremely small grain size of the nanocrystals this mismatch angle is apparently accommodated by lattice distortions and other lattice defects. Most interesting is that we can clearly see several crystal defects in the Fourier-filtered image shown in Fig. 5(b). One is the vacancy row indicated by the black arrow. The $\{111\}$ lattice planes bend strongly towards the vacancy row. A small kink in the twin boundary between variants T_1 and T_5 and a dislocation pair with an

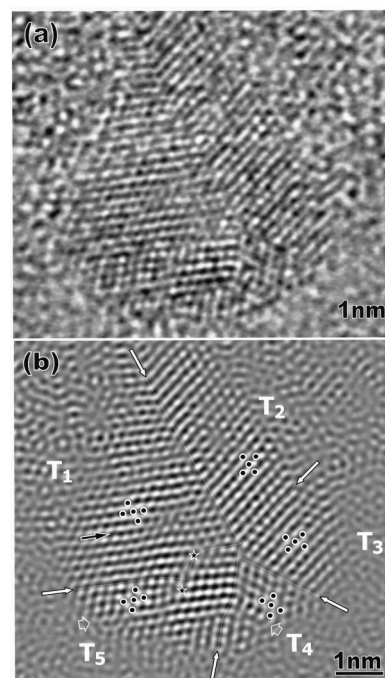


FIG. 5. Quintuplet twin structure (T_1 – T_5) in a small nanocrystal. (a) The original image. (b) Fourier-filtered image clearly showing lattice defects. The white lines mark the $\Sigma=3$ twin boundaries in the quintuplet structure. The black arrow indicates a vacancy row in the $\{111\}$ plane. Stars denote a pair of dislocations.

extremely small separation can be recognized; they are denoted by stars.

The mc diamond films are conventionally deposited via a two-step process: nucleation and growth. Due to the extremely high surface energy of diamond crystal the nucleation of diamond on a foreign substrate can only be achieved with the use of a special pretreatment such as scratching the surface with diamond particles or bombarding it with ion energy of 10–100 eV. The former is an *ex situ* process with a nucleation density of 10^8 – 10^9 cm⁻², leading to an initial grain size in submicrons. During the growth step the grain size increases continuously with the film thickness. The ion bombardment, often called bias enhanced nucleation (BEN), can, however, be performed *in situ* and transferred smoothly to the growth step. By avoiding mechanical surface damage, BEN has been successfully used to achieve the heteroepitaxy of diamond on technologically relevant substrate materials such as Si and β -SiC.¹³

BEN is performed at negative substrate voltage in the range of –80 to –250 V for 5–30 min as function of other deposition parameters, and nanometer-sized nuclei with densities of more than 10^{10} cm⁻² can form. The attraction of positively charged energetic ions due to negative bias increases the bombardment of the substrate surface, which has two effects on the substrate surface: the creation of surface lattice defects in the substrate which will serve as active nucleation sites and the enhancement of surface diffusion of adatoms. The former is beneficial for growing nc crystals and the latter will promote the coalescence of nuclei, which is an obstacle in the formation of nc films. If the substrate bias is, like in the case of this study, continuously applied at voltage of –140 V after the initial nucleation step, surface defects, including surface graphitization of the growing diamond crystal surface, may be produced which interrupt homoepitaxial growth of the diamond crystals and lead to high frequency secondary nucleation. The growth of the existing nuclei cannot then proceed and films with nc structure are prepared. Taking the growth rate of 3.72 nm/min and the average grain size of 8 nm into account and assuming a linear crystal growth law, a rate of secondary nucleation of 7.3×10^{11} cm⁻² min⁻¹ can be estimated, which is much higher than that of BEN nucleation on Si, 1.1×10^{10} cm⁻² min⁻¹, neglecting the incubation time.¹⁴

Regarding the small grain size, the lattice defect density shown in Figs. 4 and 5 is extremely high, indicating that more lattice defects are generated at the nucleation stage than that at the grain growth stage. This concentration phenomenon can be ascribed to the low activation barrier of defect creation and the high number of surface vacancies due to ion impact during grain growth. Due to the high surface/volume

ratio of nanocrystals the cluster lattice can easily become deformed. The linear crystal defects result in lattice strain of several tens of nanometers and the lattice deformation energy rises rapidly with the grain size.¹⁵ For nanometer-sized crystals the defect formation barrier is low because small amounts of lattice strain energy will be stored. As a result of ion impact, the surface structure will be modified. H⁺ ions etch as-grown C particles and form surface vacancies which can diffuse onto the surface.^{6,16} Ion impact may enhance the accumulation of vacancies in the crystal, forming a flank-type dislocation loop.

In summary, the synthesis of diamond nanocrystals was demonstrated by different methods. The MWCVD process assisted by continuous ion bombardment leads to high-frequency secondary nucleation and the formation of nanometer-sized crystals. Investigations of the microstructure and the defects were performed. Due to the small grain size and ion bombardment the nanocrystals grown show a much higher density of crystal defects and larger lattice distortions in comparison to microcrystals. The adhesion of the films to the silicon substrate is reasonably good for film thickness smaller than 2 μ m. Due to the high amount of compressive stress in the film, thicker films are seldom prepared.

This work was partially supported by NEDO and by JFCC as part of the Frontier Carbon Technology (FCT) project promoted by AIST, MITI, Japan.

¹Special edition, MRS Bull. **24** (1999).

²D. M. Gruen, S. Liu, A. R. Krauss, J. Luo, and X. Pan, Appl. Phys. Lett. **64**, 1502 (1994).

³L. C. Qin, D. Zhou, A. R. Krauss, and D. M. Gruen, Nanostruct. Mater. **10**, 649 (1998).

⁴D. M. Gruen, MRS Bull. **9**, 32 (1998).

⁵S. A. Catledge and Y. K. Vohra, J. Appl. Phys. **86**, 698 (1999).

⁶X. Jiang, W. J. Zhang, and C.-P. Klages, Phys. Rev. B **58**, 7064 (1998).

⁷X. Jiang, C. Z. Gu, L. Schäfer, and C.-P. Klages, Proceedings of ADC/FCT'99, edited by M. Yoshikawa, Y. Koga, Y. Tzeng, C.-P. Klages, and K. Miyoshi, 3 September 1999, Tsukuba, Japan, p. 28.

⁸C. Z. Gu and X. Jiang, J. Appl. Phys. **88**, 1788 (2000).

⁹C. Z. Gu, X. Jiang, and Z. Jin, J. Vac. Sci. Technol. B **19**, 962 (2001).

¹⁰N. Jiang, K. Sugimoto, K. Eguchi, T. Inaoka, Y. Shintani, H. Makita, A. Hatta, and A. Hiraki, J. Cryst. Growth **222**, 591 (2001).

¹¹D. Shechtman, A. Feldman, M. D. Vaudin, and J. L. Hutchison, Appl. Phys. Lett. **62**, 487 (1993); D. Shechtman, A. Feldman, and J. L. Hutchison, Mater. Lett. **17**, 211 (1993).

¹²J. Narayan, J. Mater. Res. **5**, 2414 (1990).

¹³X. Jiang and C. L. Jia, Phys. Rev. Lett. **84**, 3658 (2000).

¹⁴X. Jiang, K. Schiffmann, and C.-P. Klages, Phys. Rev. B **50**, 8402 (1994).

¹⁵J. Michler, Y. von Kaenel, J. Stiegler, and E. Blank, J. Appl. Phys. **83**, 187 (1998).

¹⁶M. Franklath, S. Skokov, and B. Weiner, *Electrochemical Society Proceedings*, 1995, Vol. 95-4, p. 1.